



Real-time, fast radio transient searches with GPU de-dispersion

A. Magro,¹★ A. Karastergiou,² S. Salvini,³ B. Mort,³ F. Dulwich³
and K. Zarb Adami^{1,2}

¹Department of Physics, University of Malta, Msida MSD 2080, Malta

²Astrophysics, University of Oxford, Denys Wilkinson Building, Keble Road, Oxford OX1 3RH

³Oxford e-Research Center, University of Oxford, 7, Keble Road, Oxford OX1 3QG

Accepted 2011 July 12. Received 2011 July 11; in original form 2011 April 15

ABSTRACT

The identification and subsequent discovery of fast radio transients using blind-search surveys require a large amount of processing power, in worst cases scaling as $\mathcal{O}(N^3)$. For this reason, survey data are generally processed off-line, using high-performance computing architectures or hardware-based designs. In recent years, graphics processing units (GPUs) have been extensively used for numerical analysis and scientific simulations, especially after the introduction of new high-level application programming interfaces. Here, we show how GPUs can be used for fast transient discovery in real time. We present a solution to the problem of de-dispersion, providing performance comparisons with a typical computing machine and traditional pulsar processing software. We describe the architecture of a real-time, GPU-based transient search machine. In terms of performance, our GPU solution provides a speed-up factor of between 50 and 200, depending on the parameters of the search.

Key words: instrumentation: miscellaneous.

1 INTRODUCTION

One of the most ambitious experiments of the next-generation radio telescopes, such as the newly inaugurated Low Frequency Array (LOFAR) and the future Square Kilometre Array (SKA), is to explore the nature of the dynamic radio sky at time-scales ranging from nanoseconds to years (Stappers et al. 2011). Surveys for very fast radio transients necessarily generate huge amounts of data, making storage and off-line processing an unattractive solution. However, real-time processing offers the possibility to react as fast as possible and to conduct follow-up observations across the electromagnetic spectrum and even, for some events, with gravitational wave detectors. Here, we consider the case where time-series data (tied-array, or beam-formed data for the array telescopes mentioned above) are processed to extract astrophysical radio bursts of short duration. Cordes & McLaughlin (2003) have discussed the multitude of potential astrophysical events that can produce such transients, ranging from individual pulses from neutron stars to Lorimer bursts (Lorimer et al. 2007).

In this paper, we are mostly concerned with de-dispersion. This refers to a family of techniques employed to reverse the frequency-dependent refractive effect of the interstellar medium (ISM) on the radio signals passing through it. We also use interstellar scattering to constrain the parameter space of a given search (see Lorimer & Kramer 2005, chapter 4, for more details on these effects). From pulsar studies, it is well determined that propagation through the

ISM obeys the cold plasma dispersion law, where the time delay between two frequencies f_1 and f_2 is given by the quadratic relation

$$\Delta t \simeq 4.15 \times 10^6 \text{ ms} \times (f_1^{-2} - f_2^{-2}) \times DM. \quad (1)$$

Here, DM is the value of the dispersion measure (DM) in pc cm^{-3} and f_1 and f_2 are in MHz. Astrophysical objects have a particular DM value associated with them, which depends on the total amount of free electrons along the line of sight and, therefore, on the distance to the object from Earth.

The removal of the dispersion effect from astrophysical data is typically done in two ways, depending on the type of data and the requirements of the experiment. For total power filterbank data, where the spectral bandwidth of the observation is typically split into a number of narrow frequency channels, de-dispersion consists of a relative shift in time of all frequency channels according to equation (1). This is known as incoherent de-dispersion because it is performed on incoherent data. For baseband data, de-dispersion can be carried out by convolution of the observed voltage data with the inverse of the transfer function of the ISM. This is known as coherent de-dispersion; it is more accurate in terms of recovering the intrinsic shape of the astrophysical signal but much more demanding in computational power. In this paper, we deal with incoherent de-dispersion, applied to total power data.

De-dispersion is an expensive operation, scaling as $\mathcal{O}(N^2)$ for brute-force algorithms, with more optimized techniques diminishing this to $\mathcal{O}[N \log(N)]$. For any blind, fast transient search, de-dispersion needs to be performed over a range of DM values, practically multiplying the number of operations required by the number of DM values in the search. Typically, thousands of finely

*E-mail: lessju@gmail.com

spaced DM values need to be considered, so the entire operation becomes extremely compute-intensive. In the past, searches for fast transients, such as single-pulse pulsar searches, have been performed off-line on archival data, using standard processing tools on large computing clusters or supercomputers. The power of such searches is shown by the discovery of rotating radio transients (RRATs; McLaughlin et al. 2006).

Here, we discuss how such searches can be performed on-line by using standard off-the-shelf general purpose graphics processing units (GPUs). In recent years, with the introduction of new high-level application programming interfaces (APIs), such as CUDA (NVIDIA Corporation 2010), these devices can easily be used for offloading data-parallel, processing-intensive algorithms from the CPU. The idea of performing transient-related signal processing on GPUs is not a new idea. For example, Ait Allal et al. (2009) have created a fully working, real-time, GPU-based coherent de-dispersion set-up at the Nançay Radio Observatory. The digital signal processing library for pulsar astronomy written by van Straten and Bailes (2010) can also use GPUs for performing coherent de-dispersion, folding and detection.

Barsdell, Barnes & Fluke (2010) have analysed various foundation algorithms that are used in astronomy, and they have attempted to determine whether these can be implemented in a massively parallel computing environment. One of the algorithms they have analysed is the brute-force de-dispersion algorithm. They have suggested that this is likely to perform to high efficiency in such an environment, although they have also stated that optimal arithmetic intensity is unlikely to be achieved without a detailed analysis of the algorithm's memory access patterns. The incoherent de-dispersion algorithm has been implemented using CUDA as a test case for the Commensal Real-Time Australian SKA Pathfinder (ASKAP) Fast Transients (CRAFT) survey (see Macquart et al. 2010; Dodson et al. 2010).

2 BLIND FAST TRANSIENT SEARCH PARAMETERS

Fast transient surveys rely on a number of search parameters, which depend on the characteristics of the instruments being used and the characteristics of the target astrophysical signals (Cordes 2008). For example, a survey for dispersed fast transients can be designed using the following input parameters:

- (i) the centre frequency at which the observation is conducted;
- (ii) the frequency bandwidth;
- (iii) the number of frequency channels and channel bandwidth;
- (iv) the sampling rate at which digital data are available;
- (v) the expected signal width, which depends on the science case;
- (vi) the acceptable signal-to-noise (S/N) level of a detected signal.

Dispersion and scattering are dependent on the frequency and bandwidth at which the survey is being conducted. These help to define the boundaries of a survey as follows.

(i) The maximum DM value (DM_{\max}) can be chosen according to the maximum DM value at which there is a justified expectation to discover sources. This could be related to the Galactic coordinates of the survey, the capabilities of the hardware and also considerations related to interstellar scattering. Scattering has the effect of reducing the peak S/N of a signal, and it is related to the DM via an empirical relationship (see Bhat et al. 2004).

Table 1. An example of a subband de-dispersion survey plan. ΔSub_{DM} refers to the DM step between two successive nominal DM values, while ΔDM is the finer DM step used for creating the de-dispersed time series around a particular nominal DM value. Bin refers to the binning coefficient for a particular pass.

Pass	Low DM (pc cm ⁻³)	High DM (pc cm ⁻³)	ΔDM (pc cm ⁻³)	Bin	ΔSub_{DM} (pc cm ⁻³)
1	0.00	53.46	0.03	1	0.66
2	53.46	88.26	0.05	2	1.2
3	88.26	150.66	0.10	4	2.4

(ii) The number of frequency channels depends on the maximum acceptable channel bandwidth. This can be chosen by considering the dispersion smearing within each channel for the larger DMs in the searched DM range. Depending on the format of the data handed down by the telescope, the generation of narrower frequency channels might be desirable and necessary.

(iii) The de-dispersion step, which is the unit of discretization of the DM range, is chosen according to the width of the target astrophysical signals and the permissible S/N loss that occurs when de-dispersing at a slightly erroneous DM.

De-dispersion itself can be performed by a brute-force algorithm, introducing time shifts to every channel, or using faster, approximative de-dispersion algorithms. Subband de-dispersion is a technique used by PRESTO¹ (Ransom 2001), and it relies on the fact that adjacent DM values often reuse the same time samples to create the de-dispersed time series. The entire band is split into a number of groups of channels, or subbands. Each subband is de-dispersed, according to a set of coarsely spaced DM values, and collapsed into a single frequency channel, representative of the band. The reduced number of pre-processed channels are then de-dispersed using a much finer DM step, resulting in de-dispersed time series for all DMs within the search range. This technique results in a slight sensitivity loss, but greatly decreases the processing time. Subband de-dispersion requires additional parameters, which in PRESTO are provided as a survey plan. This dictates how the DM range is split into 'passes', where each pass will bin the data using a different binning factor (the larger the DM, the more the signal will be smeared in time, and thus we can reduce the computational cost by averaging samples). For each pass, the DM range is partitioned, each range being ΔSub_{DM} apart. This value dictates the subband DM step between consecutive nominal DM values. The DM step is then used to split each of these partitions.

Table 1 provides an example of such a survey plan for a DM range of 0–150.66 as produced by DDPLAN, a script included with PRESTO, which generates the survey parameters by trying to minimize the smearing induced by the splitting of the bandwidth into subbands. This smearing is the additive effect of the smearing over each channel, each subband, the full bandwidth and the sampling rate (assuming the worst-case DM error).

3 GPU-BASED DE-DISPERSION

Using the CUDA API, we have implemented incoherent de-dispersion, which works on any CUDA-capable GPU attached to a host computer. Our modular code parallelizes the host and GPU

¹ PRESTO is the name of the pulsar search and analysis software developed by Scott Ransom.

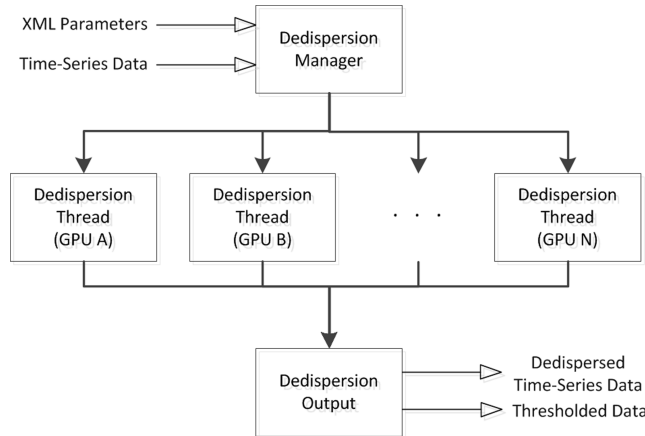


Figure 1. The high-level thread hierarchy. The de-dispersion manager initializes the entire system and then takes care of reading input data. A de-dispersion thread per GPU is created, which handles all memory copying and kernel launches on that GPU. The de-dispersion output thread then receives the de-dispersed time series from all the GPUs and performs a simple burst search.

execution by using multiple threads during the input, processing and output parts. While the input thread is reading data, the GPU is busy de-dispersing a previously read buffer and the output thread is post-processing a de-dispersed time series. This threaded set-up is depicted in Fig. 1.

The de-dispersion manager is the main thread that takes care of initializing and synchronizing the rest of the application. The input thread handles all CUDA-related calls, and an instance for each attached GPU is created. The DM range is split among these threads, such that each will process the same input buffer for different DM values. The de-dispersed output from GPU memory is then copied to host memory, to an address that is shifted appropriately to accommodate all the input threads.

The output thread constructs the de-dispersed time series and outputs the results to a data file. It can also be responsible for event detection. The simplest approach is then to calculate the mean (μ) and standard deviation (σ) for the entire processed buffer, and to use these values to apply a threshold at a particular multiple of the standard deviation ($n\sigma$). All values above the threshold are output to file as a list of triplets of the form (time, DM, intensity).

Currently, a homogeneous system is assumed, and no load-balancing between the devices is performed. Each thread is split into three conceptual ‘processing stages’, which are guarded by several thread-synchronization mechanisms. This set-up is shown in Fig. 2. The three stages are as follows: (i) the input section, where the thread inputs data to be processed; (ii) the processing section, which contains the de-dispersion kernel and which is the main section in the thread and the part that takes the longest to complete; (iii) the output section, where the processed buffer is output and made available to the next thread and any parameter updates are performed.

The two aforementioned de-dispersion techniques have been implemented, namely brute-force and subband de-dispersion, which between them have some common elements, as follows.

Maximum shift. In a buffer containing n_{samp} samples to process with a non-zero DM value, each channel will require a certain shift, with the lower-frequency channels requiring the greatest shift. Assuming this shift is of s samples, and n_{samp} samples need to be de-dispersed, we require $n_{\text{samp}} + s$ samples to be available, where s is dependent on the DM value. Because the GPU will be de-dispersing for n_{dms} DM values at any one time, the extra samples need to cater for the maximum DM value. For reference, we use the term ‘maxshift’ (m_{shift}) for this shift, which can be calculated by manipulating equation (1):

$$m_{\text{shift}} = \frac{8.3 \times 10^6 \text{ ms} \times \Delta f \times f^{-3} \times DM_{\text{max}}}{t_{\text{samp}}} \quad (2)$$

Here, t_{samp} is in ms, DM_{max} is the maximum DM value processed on the GPU and f and Δf are in MHz.

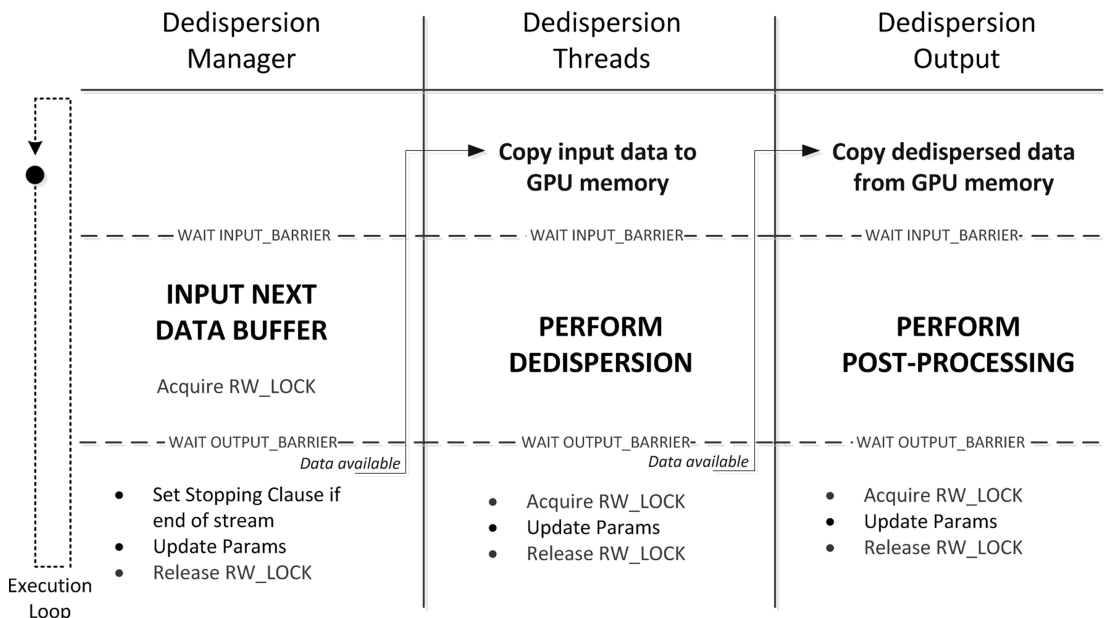


Figure 2. Each thread has three main stages: the input, processing and output stages. Data have to flow from one thread type to the next, so synchronization objects have to be used to make sure that no data are overwritten or reprocessed. Barrier and RW locks are used to control access to critical sections. See main text for a more detailed explanation.

Processable samples. Data transfers between the GPU and CPU are inefficient. For this reason, the input buffer should fill up as much of the GPU's memory as possible, leaving enough space to store the maxshift and output buffer. The simplest way to calculate the number of samples that fit in memory is

$$n_{\text{samp}} = \frac{\text{memory} - (m_{\text{shift}} \times n_{\text{chans}})}{n_{\text{dms}} + n_{\text{chans}}}. \quad (3)$$

The aim is to keep all the data within the GPU memory and to perform all processing there. So, if there are a number of operations to be performed (such as binning), n_{samp} must also accommodate these.

Shifts. Each channel requires a different amount of shift, for each DM. For an input buffer with n_{chans} channels, when de-dispersing for n_{dms} DM values, the required data structure has a size of $n_{\text{dms}} \times n_{\text{chans}}$ values. For the amount of channels and DM values required for most situations, such a data structure will not fit in constant memory, and would greatly reduce the execution speed if calculated for each block, for each DM. Storing these values in global memory would slow the kernel down. To counter this, the calculation is split into two parts, with the first part performed on the CPU

$$t_{\text{chan}} = 4.15 \times 10^3 \times (f_1^{-2} - f_2^{-2}), \quad (4)$$

where f_1 and f_2 are in MHz. This gives us a DM-independent shift for each frequency channel (i.e. the dispersion delay per unit DM), resulting in a data structure of size n_{chans} , which in normal circumstances will fit in constant memory. The second part of the calculation is then performed on the GPU:

$$t_{\text{DM}} = \frac{t_{\text{chan}} \times \text{DM}}{t_{\text{samp}}}. \quad (5)$$

The division by t_{samp} could also be performed on the CPU, but this would result in rounding errors when casting the result to single-point precision (the value on which the GPU would operate) as t_{chan} is usually very small. It is more efficient to perform the calculation on the GPU rather than using double precision throughout.

3.1 Brute-force incoherent de-dispersion

The brute-force algorithm is the simplest and most accurate to implement for de-dispersion of incoherent data, but it is also the least efficient for processing. Assuming N_s samples, each with N_c channels, and de-dispersing for N_{DM} DM values, the algorithmic time complexity of the brute-force algorithm is $\mathcal{O}(N_s \times N_c \times N_{\text{DM}})$. N_s can be seen as an infinite stream of samples, while N_c and N_{DM} will usually have similar values, resulting in approximately N^2 operations for every input sample.

According to Barsdell, Barnes & Fluke (2010), there are three main ways in which this algorithm can be parallelized: (i) N_s parallel threads each compute the sum of a single input time sample for every channel sequentially; (ii) N_c parallel threads cooperate to sum each sample in turn; (iii) $N_s \times N_c$ parallel threads cooperate to complete the entire computation in parallel. The current implementation uses a variant of scheme (i), where each thread sums up the input for a single time sample. Because of the large number of samples that can fit in GPU memory, each thread will end up processing more than one sample. A way to envisage this is to imagine the CUDA grid as a sliding window, which moves along the input samples at discrete intervals equal to the total number of threads in one row. At each grid position, threads are assigned to their respective samples.

The kernel can process any number of DM values concurrently, and this is done by creating a two-dimensional grid, where each row

is assigned a different DM value for de-dispersion. The output of the N_{DM} time series, each with N_s samples, is output to the output thread for post-processing.

This kernel is not very compute-intensive, performing fewer than 10 floating point operations per global memory read. This makes the de-dispersion algorithm memory-limited. For this reason, depending on the way the data are read from the input device, a corner-turn (matrix transpose) might be required in order to store the data in channel order. With this memory set-up, and having each thread process one sample for one DM value, threads within a half-warp (16 threads) will access the input buffer in a quasi-fully coalesced manner. This also applies for storing the result in the output buffer, because all threads within a row will shift by the same amount, resulting in stores that are also performed in a coalesced manner.

Shared memory is also used to reduce global memory reads. Each output value requires N_c additions, and performing these additions in global memory would reduce performance drastically. To counter this, each thread is assigned a cell in shared memory where the additions are performed. The final result is then copied to global memory.

3.2 Subband de-dispersion

Subband de-dispersion uses aspects of brute-force de-dispersion. However, it is also influenced by the tree algorithm, which reuses sums of groups of frequency channels for different DM values. It relies on the fact that adjacent DM values (given an appropriate DM step) will use overlapping samples during the summation. So, it splits up the DM range into several subranges, each centred around a nominal DM value. The bandwidth is also split into several subbands, resulting in a partitioning of the set of channels. The delays corresponding to the nominal DM for every channel in a subband, minus the delay at the highest frequency in that subband, are subtracted from each subband channel. This results in a partially de-dispersed set of subbands. This scheme is depicted in Fig. 3. Normal de-dispersion is then used to generate the de-dispersed time series for the rest of the DM values within the same DM subrange.

Depending on the number of subbands used, the size of the DM ranges, as well as other factors, we can limit the error induced in the result by these approximations. Further gains can be made by binning the input samples when the dispersion is so high that a pulse with a required width is smeared across multiple input samples. Binning averages N_b consecutive samples. To make our GPU code compatible with the way PRESTO generates its survey parameters, binning has also been implemented. Therefore, there are three main stages in subband de-dispersion:

- (i) perform data binning, if required;
- (ii) perform subband de-dispersion and generate the intermediary time series;
- (iii) de-disperse the resultant time series to generate the final de-dispersed time series.

Data transfers between the host and GPU are expensive, so the above stages are performed in the GPU without any data going back to the host, with appropriate data buffer re-organization performed after each kernel execution. The memory organization after each stage is depicted in Fig. 4, which can be described from top to bottom as follows.

- (i) The input buffer contains $(n_{\text{samp}} + m_{\text{shift}}) \times n_{\text{chans}}$ values.
- (ii) Binning averages N_b adjacent samples, so the output of one binning loop is $(n_{\text{samp}} + m_{\text{shift}}) \times n_{\text{chans}}/N_b$, with each loop having

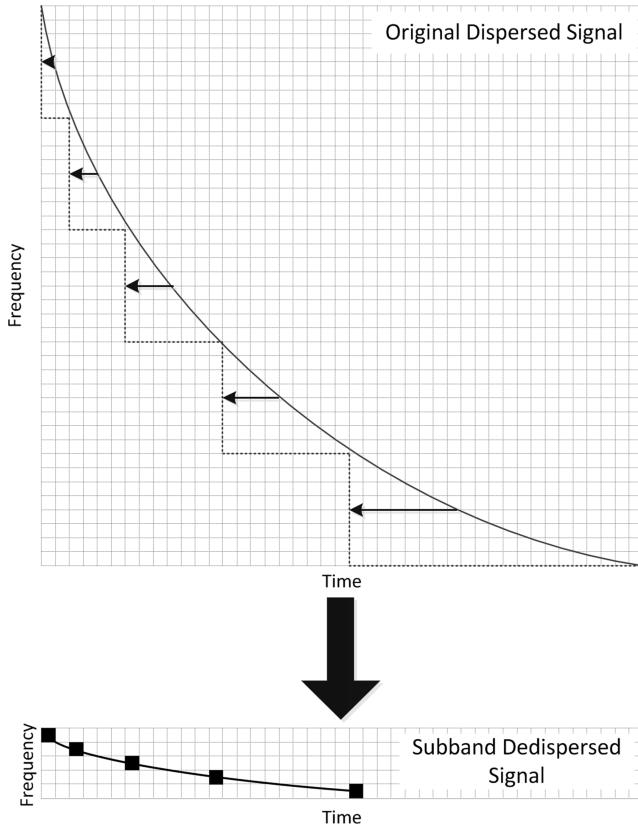


Figure 3. A simple illustration to visually depict how subband de-dispersion works. The channels are partitioned into a set of subbands where the delays corresponding to the nominal DM for every channel in the subband, minus the delay at the highest frequency in the subband, are subtracted from each channel. The subband de-dispersed signal is then further de-dispersed using normal brute-force de-dispersion for a range of DM values around the nominal DM value.

a different value for b . The output of each binning loop is placed at the tail of the previous output, as shown in the diagram. For l loops, the buffer will end up containing l logical blocks, each with a different bin size b_i . The memory, in samples, required for this procedure is

$$mem = \sum_{i=0}^l \left[\frac{(n_{\text{samp}} + m_{\text{shift}}) \times n_{\text{chans}}}{b_i} \right]. \quad (6)$$

(iii) Subband de-dispersion generates N_{sub} intermediate time series for each nominal DM, each consisting of $(n_{\text{samp}} + m_{\text{shift}})/b_i$ samples containing n_{subs} channels. Maxshift samples have to be preserved so that the next stage can process all of n_{samp} . The memory, in samples, required for this stage is

$$mem = \sum_{i=0}^l \left[\frac{(n_{\text{samp}} + m_{\text{shift}}) \times n_{\text{subs}} \times N_{\text{sub}}}{b_i} \right]. \quad (7)$$

(iv) The final output consists of the de-dispersed time series for all the DM values, each containing n_{samp}/b_i values. Thus, the memory requirement for this stage, in samples, is

$$mem = \sum_{i=0}^l \left(\frac{n_{\text{dms}} \times n_{\text{samp}}}{b_i} \right). \quad (8)$$

Having defined the input and output memory requirements for all the GPU stages, the number of samples that can be processed can

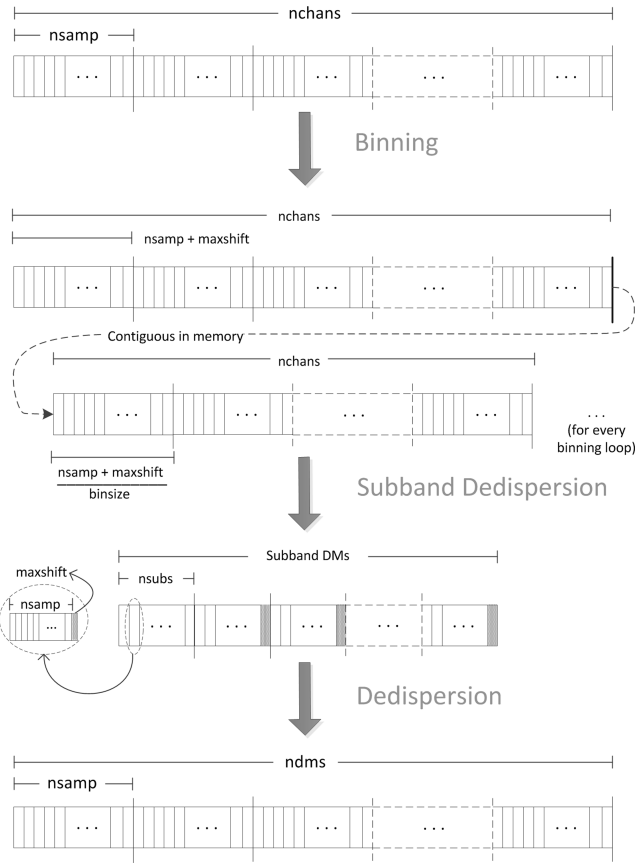


Figure 4. Subband de-dispersion requires three passes of the data: binning, subband de-dispersion and brute-force de-dispersion. During the entire process, data are kept in GPU memory, and this illustration shows how these data are organized before and after each pass.

then be calculated. The sizes of the input and output buffers can be computed by taking the size of the respective largest buffer from the processing stages, which can then be used to compute the number of samples that will fit in memory.

The subband de-dispersion kernel is very similar to the brute-force one, the only major change being that not all the channels are summed up to generate the series, and more than one value is generated per input sample. This makes the algorithm less compute-intensive and more memory-limited (the same number of input requests, more output requests). However, the number of nominal DM values is only a fraction of the total number of DM values. This greatly reduces the number of calculations that need to be performed by the brute-force algorithm.

4 RESULTS AND COMPARISONS

To test the code, a file containing a pulsed signal was generated using the fake pulsar generator within SIGPROC² (Lorimer, <http://sigproc.sourceforge.net>). The parameters used to generate this fake file are listed in Table 2. The fake filterbank data are generated as 1024 time series, one for each frequency channel. Each is made up of a square pulse of height $8\sqrt{1024} = 0.25$ and Gaussian

² SIGPROC is a software package designed to standardize the analysis of various types of fast-sampled pulsar data.

Table 2. The parameters used to generate the fake file for evaluation. A pulsar with a period of 1 s and 1 per cent duty cycle was created at a centre frequency of 153 MHz with a 6-MHz bandwidth. The bandwidth is divided into 1024 channels and a sampling time of 165 μ s was used. The DM is 75 pc cm^{-3} .

Parameter	Value
Pulsar period	1000 ms
Duty cycle	1 per cent
Pulsar DM	75.00 pc cm^{-3}
Top frequency	156.0 MHz
Channel bandwidth	5.941 kHz
Number of channels	1024
Sampling time	165 μ s

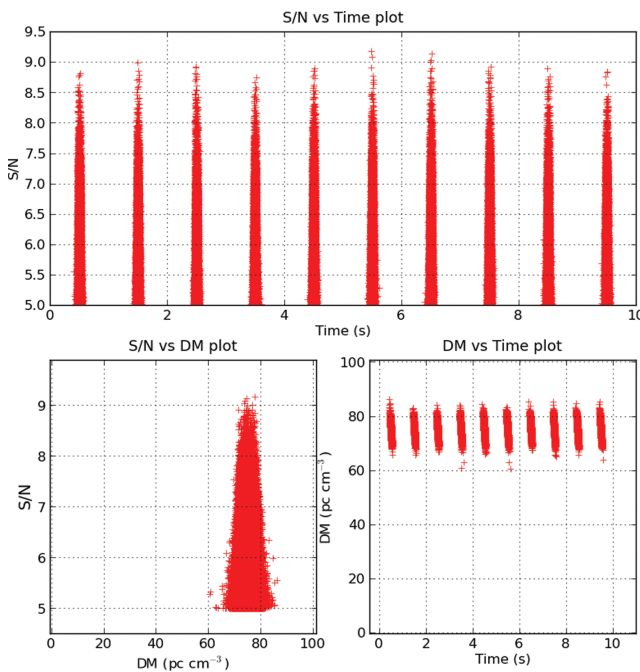


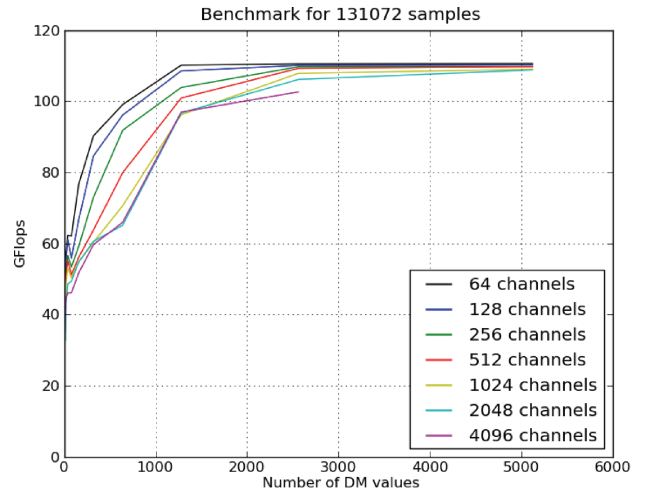
Figure 5. Brute-force de-dispersion output for an input file containing a simulated pulsar (see text for details). The plots are S/N versus time (top), S/N versus DM (bottom left) and DM versus time (bottom right). A threshold of 5σ is applied to the output. The data points shown are at the DM of the simulated pulsar, 75 pc cm^{-3} .

noise with mean 0 and standard deviation 1. The S/N of the average simulated pulse, integrated over frequency, has a mean value of 8.

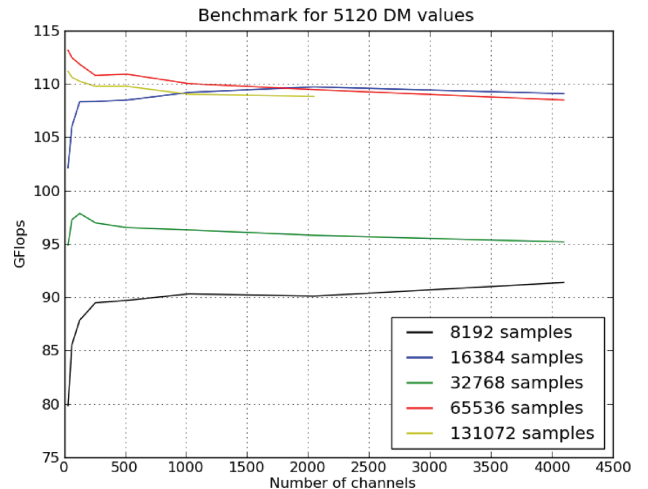
Brute-force de-dispersion using 1000 DM values with a DM step of 0.1 pc cm^{-3} was performed. Fig. 5 shows the output of the de-dispersion code, which captures all pulses with S/N greater than 5.

The performance of the CUDA implementations has been measured. Fake data are generated in the testing runs themselves, with all the elements initialized to the same value. The time taken to generate and copy the data to and from GPU memory is not included in the timings.

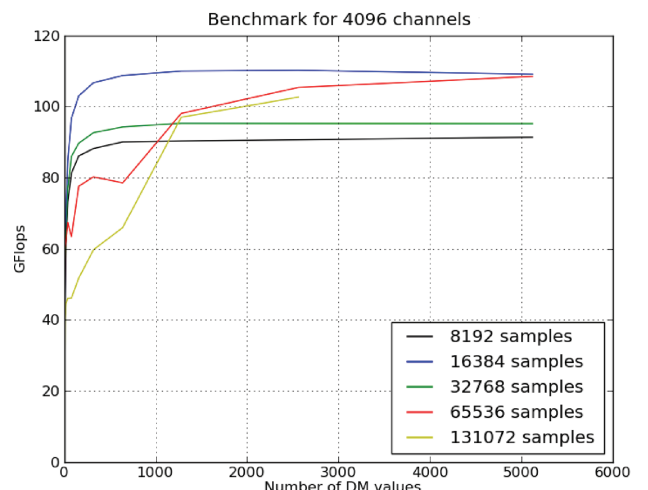
Fig. 6 shows the performance achieved when de-dispersing with different numbers of channels, samples and DM values. Different parameter configurations will result in some different optimal combinations, for example, in cases where the number of data partitions to process is exactly divisible by the number of processors and



(a) Maximum number of samples



(b) Maximum number DM values



(c) Maximum number of channels

Figure 6. Brute-force de-dispersion performance plots for a CUDA brute-force implementation. The general trend is for performance to increase linearly with increasing numbers of channels, samples and DM values, with different configurations reaching asymptotic behaviour at different peak performances. (Incomplete lines show cases where there was not enough memory on the GPU to store the data required to perform the test.)

thread blocks being used. The general tendency is for performance to increase linearly as the numbers of channels, samples and DM values increase until the maximum GPU occupancy level is reached, after which the behaviour becomes asymptotic. The optimal block size is 128, as fewer threads will result in less latency hiding and more threads will increase scheduling latency without performance benefits. The grid size does not affect performance too much, except when there are too many threads in each block.

As already stated, the de-dispersion algorithm is memory-bound, and both the GPU and CPU will spend most of their time waiting for data. For this reason, the flop rate achieved on the GPU is a small percentage of the theoretical peak for the C1060, between 80 and 120 Gflops, which is about 15–20 per cent. The memory bandwidth achieved within the GPU is about 55 GB s^{-1} , which is about 50 per cent of the theoretical peak.

The same tests were performed on a CPU, specifically on one core of a QuadCore Intel Xeon 2.7 GHz. CPU performance decreases quasi-linearly as the numbers of samples or channels increase because of cache misses. This performance is then compared with the appropriate GPU performance to produce the comparison plots in Fig. 7. This shows the speed-up gained in performing brute-force de-dispersion when using GPUs, for different parameter values. From these plots, it follows that, on average, we obtain a speed-up of about two orders of magnitude, between $50\times$ and $200\times$, depending on the parameters used, with the speed-up increasing as the numbers of input samples/channels increase.

The CUDA implementation was then compared to the two most commonly used de-dispersion scripts, the one in PRESTO and the one in SIGPROC. A fake file was generated containing a 600-s observation centred at 153 MHz with a bandwidth of 6.24 MHz split into 1024 channels and having a sampling rate of 165 ms (containing a total of about 3.6×10^6 samples). This was run through the three software suites for a single DM value. For the GPU code and PRESTO only the actual de-dispersion part was timed, whilst SIGPROC also loads from file in the innermost loop so the timing contains some file I/O times as well. The timings are listed in Table 3.

The algorithm used to perform subband de-dispersion (both steps) is almost identical to the one used in brute-force de-dispersion, so the scaling tests were not repeated. Fig. 8 depicts a comparison plot between the two algorithms for various de-dispersion parameters. The speed-up factor depends on optimal parameter combinations as well as the number of subbands and the number of nominal DM values in the DM range employed for subband de-dispersion. The speed-up factor decreases linearly with an increasing number of nominal DM values for a particular range, because more work needs to be done in the first algorithm step (although the same numbers of DM values are processed, the first step will generally be more intensive because the data have not yet been reduced). The number of nominal DM values and the number of subbands depend on the amount of dispersion smearing permissible, where a large subband–DM step and a few subbands result in a higher amount of smearing. These values should be fine-tuned to acquire the best balance between S/N and processing speed.

The GPU subband de-dispersion implementation was also compared with PRESTO's prepsubband script, on which the algorithm is based. A fake file was created for a single-beam 60-s observation at 300 MHz with a bandwidth of 16 MHz and 1024 channels. The plan used for the test is listed in Table 4. The times taken for the GPU code and PRESTO to process the entire file are 90 and 7540 s, respectively. Again, this indicates that the GPU code is about two orders of magnitude faster than the CPU implementation, in this case $84\times$ faster. For this test, PRESTO was run in single-thread mode.

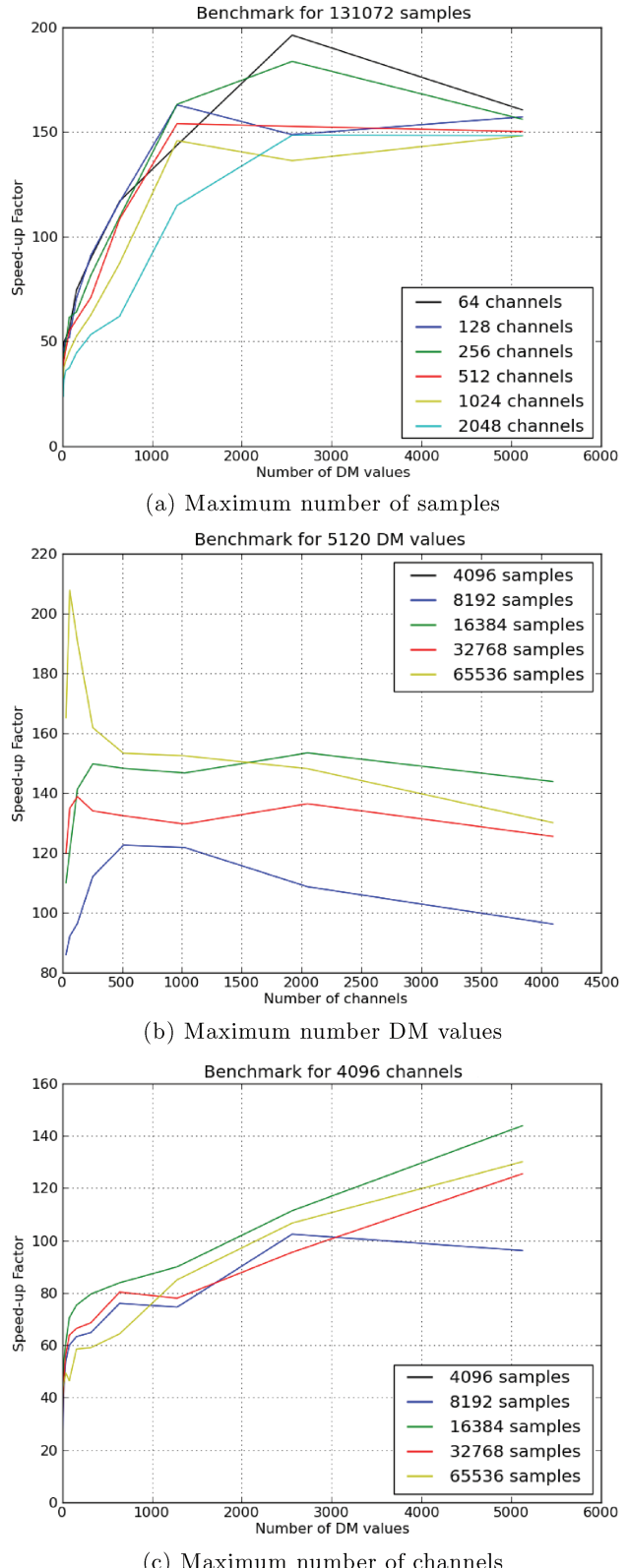
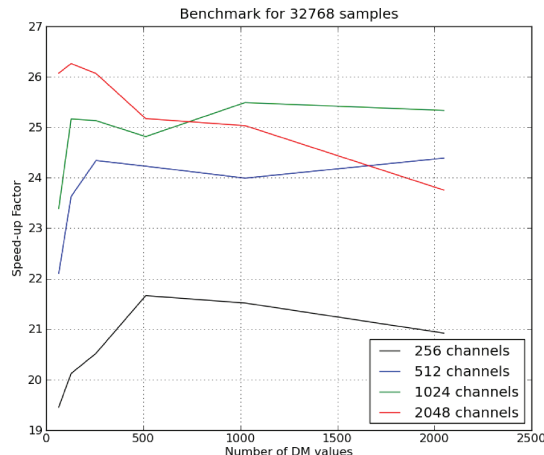


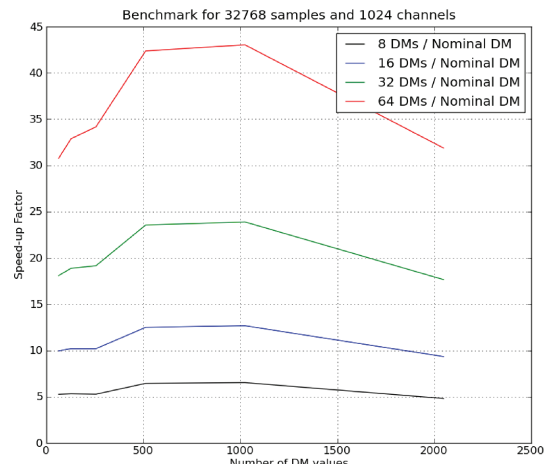
Figure 7. Brute-force de-dispersion speed-up plots. For the maximum number of samples used in the tests (a), the performance speed-up converges to about $150\times$, with peaks at different numbers of channels for different numbers of DM values. For the maximum number of DM values (b), the speed-up decreases quasi-linearly with increasing numbers of channels because of maxshift offset. For the maximum number of channels (c), performance increases quasi-linearly.

Table 3. Timing comparison between the GPU code, PRESTO and SIGPROC for one DM. SIGPROC loads data in its innermost loop so some of the time listed is actually spent reading from file. The timing discrepancy between the GPU code and PRESTO is consistent with the speed-up plots.

Suite	Timing
GPU code	0.257 s
PRESTO	28.321 s
SIGPROC	58.099 s



(a) The speed up of subband versus brute force de-dispersion



(b) Different DM values per nominal DM in subband de-dispersion

Figure 8. The relative speed up of subband de-dispersion compared to brute-force de-dispersion on the GPU. (a) A comparison of a series of de-dispersion runs with varying parameters using the two algorithms. The speed-up factor depends on optimal parameter combinations, the number of subbands and the number of DM values per nominal DM used to split the DM range, as shown in (b). See main text for further details.

5 REAL-TIME DE-DISPERSION

The performance boost obtained from GPUs makes them an ideal candidate for use in real-time systems. An off-the-shelf server with

Table 4. Subband de-dispersion survey plan used to compare PRESTO and the GPU code, for a 60-s observation at 300 MHz with a bandwidth of 16 MHz split across 1024 channels.

Pass	Low DM (pc cm ⁻³)	High DM (pc cm ⁻³)	ΔDM (pc cm ⁻³)	Bin	ΔSub_{DM} (pc cm ⁻³)
1	0.00	53.46	0.03	1	0.66
2	53.46	88.26	0.05	2	1.2
3	88.26	150.66	0.10	4	2.4

a high-end CUDA-enabled graphics card has enough power to de-disperse thousands of DM values in real time (depending on telescope parameters). Additional features are required for such a system, such as a way to read and interpret incoming telescope data and further channelization and buffering between the input stream and de-dispersion buffers.

As a proof of concept, the GPU code was extended to include a channelizer (a simple FFT using the NVIDIA CUFFT library) and a kernel to calculate the power from incoming complex voltages, in order to simulate the situation of attaching such a machine to a baseband recorder. This was used within a broader application, which (i) reads in UDP packets, filling up buffers within a double-buffer framework, (ii) forwards filled buffers to the GPU code, (iii) channelizes and calculates total power, (iv) transposes data so that it is in channel order and (v) performs de-dispersion. A UDP data emulator was used to create a simulated voltage stream from the SIGPROC fake data files and to send them to the processing pipeline. This set-up is shown in Fig. 9.

A fake observation file was generated, whose parameters (defined in Table 5) were large enough that multiple iterations of the pipeline would be required, together with the processing parameters. The brute-force de-dispersion algorithm was used for the test. Note that the data emulator's output speed will not match the simulated telescope's output data rate, so the way to determine whether the pipeline is processing in real time is to time how long the GPU takes to process one entire buffer, and then to compare that with the number of samples originally buffered.

The GPU buffer sizes were set to 2^{19} spectra, equivalent to about 6.7 s of telescope data. This means that all the GPU processing for each buffer must complete within this time frame. The average timings for each stage of the pipeline are listed in Table 6. The total processing time on an NVIDIA C1060 card is about 5.8 s. This leaves enough extra time for CPU–GPU synchronization and additional memory operations, also providing enough leeway for the occasional CPU processing burst as a result of other running processes or the OS itself. The test was run on server with two QuadCore Intel Xeon 2.7 GHz and 12 GB DDR3 RAM, which is a modest system for on-line processing.

6 CONCLUSIONS

We have implemented two de-dispersion algorithms, brute-force and subband de-dispersion, using CUDA, which enables data-parallel processing to be offloaded on to any number of connected CUDA-enabled GPUs. This has led to a performance speed-up of about two orders of magnitude, between 50 and 200 for certain parameter configurations, when compared to a single-threaded CPU implementation. A detailed comparison with two traditional pulsar processing suites, PRESTO and SIGPROC, confirms our results. Finally, a prototype for a real-time dispersion search pipeline was designed,

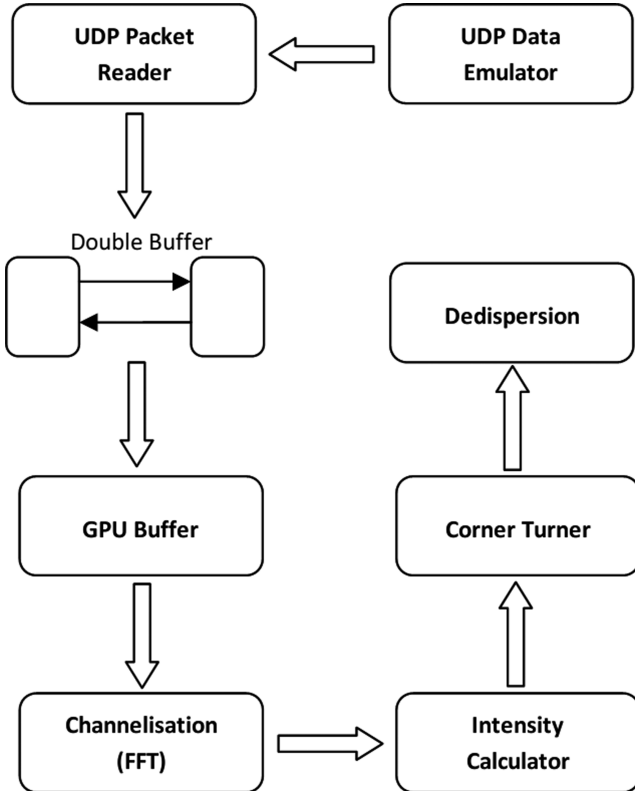


Figure 9. A set-up for real-time de-dispersion. The UDP Data Emulator packetizes SIGPROC files and sends the data through UDP to the processing pipeline, where the packets are read, interpreted and stored in a double buffer. Once a buffer is full, it is forwarded to the GPU, which performs channelization, power calculation, a corner turn and de-dispersion.

Table 5. The parameters of the observation file generated to test the real-time pipeline. The fake file was generated with an observation at a centre frequency of 610 MHz and a 20-Mhz bandwidth with 256 channels, producing 78 125 spectra per second. The channelizer produces eight channels per subband, and 500 DM values are used for the dispersion search, with a maximum DM of 60 pc cm^{-3} .

Parameter	Value
Centre frequency	610 MHz
Bandwidth	20 MHz
Number of subbands	256
Sampling time	12.8 μs
Channels per subband	8
Number of DM values	500
Maximum DM value	60 pc cm^{-3}

which reads in a UDP stream of telescope data and performs FFT channelization and de-dispersion.

Work is ongoing in this project, with plans to add several additional processing modules in the pipeline. Coherent de-dispersion

Table 6. Timings for the various stages in the processing pipeline.

Stage	Time
CPU to GPU copy	475 ms
Channelization	458 ms
Intensity calculation	20 ms
Corner turn	112 ms
De-dispersion	4500 ms
GPU to CPU copy	220 ms
Total	5785 ms

is useful for studying pulsars whose DM value is already known. Other schemes for de-dispersion are also being considered, such as performing chirp analysis in the frequency domain to detect chirps representing dispersed signals. GPUs provide us with enough processing power (per unit cost) to be able to apply processing-intensive algorithms, which would otherwise be unfeasible on a conventional CPU system. As a result, we are in a position to carry out real-time searches for dispersed fast transients with appropriate telescopes at low cost.

ACKNOWLEDGMENTS

The research work disclosed in this publication is partially funded by the Strategic Educational Pathways Scholarship (Malta). AK is grateful to the Leverhulme Trust for financial support. We thank the referee, Scott Ransom, for a constructive review of the paper.

REFERENCES

- Ait-Allal D., Weber R., Cognard I., Desvignes G., Theureau G., 2009, in Proc. 17th European Signal Processing Conference (EUSIPCO), p. 2052
- Barsdell B., Barnes D., Fluke C., 2010, MNRAS, 408, 1936
- Bhat N. D. R., Cordes J. M., Camilo F., Nice D. J., Lorimer D. R., 2004, ApJ, 605, 759
- Cordes J. M., 2008, in Bridle A. H., Condon J. J., Hunt G. C., eds, ASP Conf. Ser. Vol. 395, Frontiers of Astrophysics: A Celebration of NRAO's 50th Anniversary. Astron. Soc. Pac., San Francisco, p. 225
- Cordes J. M., McLaughlin M. A., 2003, ApJ, 596, 1142
- Dodson R., Harris C., Pal S., Wayth R., 2010, in Proceedings of Science, ISKAF2010 Science Meeting, <http://pos.sissa.it/cgi-bin/reader/conf.cgi?confid=112>
- Lorimer D. R., Kramer M., 2005, Handbook of Pulsar Astronomy. Cambridge Univ. Press, Cambridge
- Lorimer D. R., Bailes M., McLaughlin M. A., Narkevic D. J., Crawford F., 2007, Sci, 318, 777
- McLaughlin M. A. et al., 2006, Nat, 439, 817
- Macquart J. P. et al., 2010, PASA, 27, 272
- NVIDIA Corporation, 2010, cuda Zone, http://www.nvidia.com/object/cuda_home_new.html
- Ransom S., 2001, PhD thesis, Harvard University, Cambridge, MA
- Stappers B. W. et al., 2011, A&A, 530, A80
- van Straten W., Bailes M., 2011, PASA, 28, 1

This paper has been typeset from a $\text{\TeX}/\text{\LaTeX}$ file prepared by the author.